Form No. 24

Search for new physics in the charged lepton sector

(JINR participation)

Project extension for the period 2022-2024

02-2-1144-2021/2023 Search for new physics in the charged lepton sector

G.Adamov[1], A.M.Artikov[1], D.Aznabayev[3], D.Baigarashev[2], A.V.Boikov[1], D.Chokheli[1], Yu.I.Davydov[1], V.N.Duginov[1], T.L.Enik[2], I.L.Evtoukhovitch[1], P.G.Evtoukhovitch[1], V.V.Glagolev[1], D.Goderidze[4], A.Issadykov[3], V.A.Kalinnikov[1], E.S.Kaneva[1], X.Khubashvili[1], A.Khvedelidze[4], A.Kobey[1], G.A.Kozlov[3], A.S.Moiseenko[1], A.V.Pavlov[1], B.M.Sabirov[1], A.G.Samartsev[1], A.V.Simonenko[1], V.V.Tereschenko[1], S.V.Tereschenko[1], Z.Tsamalaidze[1], N.Tsverava[1], I.I.Vasilyev[1], E.P.Velicheva[1], A.D.Volkov[1], I.Yu.Zimin[1]

[1]Dzhelepov Laboratory of Nuclear Problems (DLNP)
[2]Veksler and Baldin Laboratory of High Energy Physics (VBLHEP)
[3]Bogoliubov Laboratory of Theoretical Physics (BLTP)
[4]Laboratory of Information Technologies (LIT)

Project leaders: **V.V.Glagolev, Z.Tsamalaidze**

Scientific Project leader: **Yu.A.Budagov**

DATE OF SUBMISSION OF PROPOSAL OF PROJECT TO SOD: _____

DATE OF THE LABORATORY STC: **01.04.2021** DOCUMENT NUMBER: _____

STARTING DATE OF PROJECT: **2022**

(FOR EXTENSION OF PROJECT — DATE OF ITS FIRST APPROVAL): **2015**

Date of the Lab seminar: **10.03.2021**

Form No. 25

PROJECT ENDORSEMENT LIST

Search for new physics in the charged lepton sector

(JINR participation)

Project extension for the period 2022-2024

02-2-1144-2021-2023 Search for new physics in the charged lepton sector

V.V.Glagolev, Z.Tsamalaidze

APPROVED BY JINR DIRECTOR		
ENDORSED BY		
JINR VICE-DIRECTOR		
CHIEF SCIENTIFIC SECRETARY		
CHIEF ENGINEER		
HEAD OF SCIENCE ORGANIZATION DEPARTMENT		
LABORATORY DIRECTOR		
LABORATORY CHIEF ENGINEER		
PROJECT LEADER		
ENDORSED		
RESPECTIVE PAC		

Search for new physics in the charged lepton sector

(JINR participation)

Project extension for the period 2022-2024

Contents

1. Abstract

Charged-lepton flavour-violating (CLFV) processes offer deep probes for new physics with discovery sensitivity to a broad array of new physics models, based on the naturally motivated extensions of the Standard Model of the elementary particles, e.g., 2 HDM, SUSY, Extra Dimensions, and, particularly, models explaining the neutrino mass hierarchy and the matter-antimatter asymmetry in the Universe via leptogenesis.

The most sensitive exploration of CLFV is provided by experiments that utilize high intensity muon beams to search for CLFV in $\mu \rightarrow e$ transitions. COMET (COherent Muon to Electron Transition) experiment at J-PARC is one of such experiments, it's aim is to search for the coherent neutrinoless conversion of a muon into an electron in the field of an aluminum nucleus $\mu^- N \rightarrow e^- N$.

COMET experiment will be realized in two phases, Phase-I [1] and Phase-II [2]. The experimental sensitivity goal for this process in the Phase-I experiment is 3.1×10^{-15}, or 90% upper limit of branching ratio of 7×10^{-15}, which is a factor of 100 improvement over the existing limit. The expected number of background events is 0.032. To achieve the target sensitivity and background level, the 3.2kW 8 GeV proton beam from J-PARC will be used. Two types of detectors, CyDet and StrECAL, will be used for detecting the μ-e conversion events, and for measuring the beam-related background events in view of the Phase-II experiment, respectively.

Scientists from JINR are participating successfully in the preparation stage of the COMET experiment. For the COMET Phase-I experiment JINR scientists produced and tested in accordance with the requirement all set of 9.8 mm straw tubes, about 2700 pcs, also participate strongly in the creation and operation of straw-tracker, electromagnetic calorimeter and CRV system. The contribution to simulations with further data analysis are also in charge.

The concurrent to the COMET experiment is the Mu2e experiment [3] at the Fermi National Accelerator Laboratory (FNAL, USA) has the same goal of search for $\mu^- \rightarrow e^-$ conversion. The muon beam line and detector for the Mu2e experiment are similar to COMET. Their planned single-event sensitivity (SES) is 3×10^{-17} (what is equivalent to the goal of COMET) with 3 years of 2×10^7 second running per year, although COMET needs only less than 1 year. While the main structure of the experimental setup is similar to COMET, there are some differences in the beamline shape (S-shape in Mu2e vs C-shape in COMET), calorimeter structure etc. The Mu2e experiment would strongly compete with the COMET experiment.

During the 2015 – 2021 period of the project COMET at JINR, 23 papers with significant participation of JINR scientists were published, more than 22 talks at international conferences and meetings were presented. The requested project budget is 690 k$ for 2022-2024.

2. Introduction

Charged-lepton flavour-violating (CLFV) processes provide unique discovery potential for physics beyond the Standard Model (BSM). These CLFV processes explore new physics parameter space in a manner complementary to the collider, dark matter, dark energy, and neutrino physics programmes.

Current limits for CLFV $\mu \rightarrow e$ transitions are in the 10^{-12} – 10^{-13} range and probe effective new physics mass scales above 10^3 TeV/c^2. Next-generation experiment COMET expects to improve these sensitivities by as much as two orders of magnitude on the timescale at 2023-2024 in Phase-I, and four orders at 2026-2027 in Phase-II. This dramatic improvement in sensitivity offers genuine discovery possibilities in a wide range of new physics models with SUSY, Extra Dimensions, an extended Higgs sector, lepto-quarks, or those arising from GUT models.

Beginning in the latter half of the next decade, upgrades to the beamline at J-PARC offer the possibility to further explore this parameter space. Improvements in sensitivity by an additional factor of 10-100 are possible with an increased intensity at J-PARC to enable an upgraded COMET (Phase-II). Significant JINR team participation in the design, construction, data taking, and analysis will be important to the success of this experiment and represents a prudent investment complementary to searches at colliders.

More specific plans for the COMET experiment is to participate hard in design and creation of the straw tracker stations with 9.8 mm straw for COMET phase-I; participate in LYSO crystals QA tests; participation in the CRV R&D, design and construction; assemble and maintenance of the COMET setup; participation in shifts, simulation and data analysis; R&D and production of the 5 mm straw for 1-st and 2-nd phases of COMET experiment.

3. State-of-the-art of this scientific problem

Historically, flavour-changing neutral currents have played a significant role in revealing details of the underlying symmetries at the foundation of the SM. In the SM there is no known symmetry that conserves lepton flavour. The discoveries of quark mixing and neutrino mixing, each awarded Nobel Prizes, provided profound insights to the underlying physics. Motivated by these past successes, there exists a global programme to explore CLFV processes providing deep, broad probes of BSM physics.

The objective is to search for evidence of new physics beyond the SM using CLFV processes in the muon sector. These processes offer powerful probes of BSM physics and are sensitive to effective new physics mass scales of 10^3-10^4 TeV/c^2, well beyond what can be directly probed at colliders. Over the next years, currently planned experiments in Europe, the US, and Asia will begin taking data and will extend the sensitivity to CLFV interactions by orders of magnitude. Further improvements are possible and new or upgraded experiments are being considered that would utilize upgraded accelerator facilities at J-PARC, PSI, and Fermilab and could begin taking data in the 2023-2027 timeframe.

Flavour violation has been observed in quarks and neutrinos, so it is natural to expect flavour violating effects among the charged leptons as well. In fact, once neutrino mass is introduced, the SM provides a mechanism for CLFV via lepton mixing in loops. However, the rate is suppressed by factors of $\left(\Delta m_{ij}^2 / M_w^2\right)^2$, where Δm_{ij}^2 is the mass difference squared between i^{th} and j^{th} neutrino mass eigenstates, compared to the mass of W-boson m_w^2, and is estimated to be extremely small, for example BF ($\mu \rightarrow e\gamma$) ~ 10^{-54} [4]. Many extensions to the SM predict large CLFV effects that

could be observed as new experiments begin data taking over the next five years. Significant improvements are expected across a wide variety of CLFV processes (e.g. $\tau \rightarrow \mu\mu\mu$, $\mu\gamma$, or $e\gamma$; $\mu \rightarrow e\gamma$, eee; $\mu N \rightarrow eN$; Z or $H^0 \rightarrow e\mu$, $e\tau$, or $\mu\tau$; $K_L \rightarrow e\mu$). The largest improvements are expected in experiments that search for CLFV transitions using muons.

Experimentally, there are three primary muon-to-electron transitions used to search for CLFV: a muon decaying into an electron plus a photon, $\mu^+ \rightarrow e^+\gamma$; a muon decaying into three electrons, $\mu^+ \rightarrow e^+e^-e^+$; and direct muon-to-electron conversion via an interaction with a nucleus, $\mu^-N \rightarrow e^-N$. These three $\mu \rightarrow e$ transitions provide complementary sensitivity to new sources of CLFV since the observed rates will depend on the details of the underlying new physics model. For example, for models in which CLFV rates are dominated by γ-penguin diagrams, the $\mu \rightarrow e\gamma$ transition rate is expected to be ~ 10^2 times larger than that of the $\mu \rightarrow eee$ and $\mu N \rightarrow eN$ rates. On the other hand, if the CLFV rates are dominated by Z- or H-penguin diagrams, or if tree level contributions are allowed (e.g., as in some lepto-quark or Z' models), then the $\mu \rightarrow e\gamma$ rate is suppressed and $\mu \rightarrow eee$ and $\mu N \rightarrow eN$ rates can instead be the largest. Thus, a programme with experiments exploring all three muon CLFV transitions maximizes the discovery potential and offers the possibility of differentiating among various BSM models by comparing the rates of the three transitions [5], [6].

Searches for $\mu \rightarrow e$ transitions have been pursued since 1947 when B. Pontecorvo and Hincks [7] first searched for the $\mu \rightarrow e\gamma$ process. Since then, the sensitivity has improved by eleven orders of magnitude via a series of increasingly challenging experiments. The current best limits for the three $\mu \rightarrow e$ transitions are BF ($\mu^+ \rightarrow e^+\gamma$) < 4.2×10^{-13} [8], BF ($\mu^+ \rightarrow e^+e^-e^+$) < 1×10^{-12} [9], $R_{\mu e}$ (Au) < 7×10^{-13} [10] at 90% CL, where $R_{\mu e}$ is the $\mu \rightarrow e$ conversion rate normalized to the rate of ordinary muon nuclear capture. Currently planned experiments will provide sensitivities well beyond these existing limits. The MEG experiment at PSI has recently completed an upgrade and expects to extend the $\mu^+ \rightarrow e^+\gamma$ sensitivity by about an order of magnitude. The COMET experiment under construction at J-PARC will extend the sensitivity to $\mu^-N \rightarrow e^-N$ by about two orders of magnitude by the early-2024s at Phase–I and four orders at Phase–II in 2025-2026.

As the charged counterpart of neutrino oscillations, CLFV plays a significant role in most of the BSM models seeking to explain the neutrino mass hierarchy and the Universe's matter anti-matter asymmetry generated through leptogenesis. The CLFV measurements thus have considerable synergy with the neutrinoless double beta decay and neutrino oscillation research programmes. For example, there is a large class of models (see e.g. [11]) proposed to explain the smallness of the neutrino mass. These typically involve extensions to the Higgs sector and the existence of heavier neutrino partners, the properties of which - sterile or non-sterile, Dirac or Majorana, and the mass-scale of the neutrino partners - depend on the model. These heavy neutrino partners typically also play a role in generating a matter anti-matter asymmetry. The majority of these models predict large CLFV effects, and the comparison of CLFV and neutrino measurements together becomes a strong constraint on the model type and its parameters. Indeed, in the most natural models, where the neutrino partners are extremely massive, these measurements are one of the few portals into GUT-scale physics. In the Inverse Seesaw models [12], right-handed neutrinos with masses in the TeV-scale are produced that are potentially observable at the LHC. The present LHC limits are below 1 TeV whereas COMET will extend this sensitivity to 2 TeV. More generally COMET till have a sensitivity for RH neutrinos up to masses of a few PeV, well beyond the direct detection limit of the LHC.

The $\mu \rightarrow e$ experiments also provide complementary information regarding the Majorana nature

of neutrinos via the $\mu^- \rightarrow e^+$ transition: $\mu^- N(Z,A) \rightarrow e^+ N(Z-2,A)$. This transition violates both lepton number and lepton flavour and can only proceed if neutrinos are Majorana. This search channel comes for “free" in the COMET experiment. The COMET sensitivity to Majorana neutrinos will significantly extend beyond the current best limit [13] with $<m_{e\mu}>$ effective Majorana neutrino mass scale sensitivity down to the MeV region surpassing the $<m_{\mu\mu}>$ sensitivity in the kaon sector which is limited to the GeV region [14].

3.1 Experimental Aspects of μ−N → e−N

The event signature of coherent neutrinoless $\mu^- \rightarrow e^-$ conversion in a muonic atom is the emission of a mono energetic single electron in a defined time interval. The energy of the signal electron ($E_{\mu e}$) is given by

$$E_{\mu e} = m_\mu - B_\mu - E_{recoil,} \quad (1)$$

where m_μ is the muon mass, B_μ is the binding energy of the 1*s*-state muonic atom, and E_{recoil} denotes the nuclear recoil energy which is small. For aluminium $E_{\mu e}$ = 104.97 MeV and the lifetime of the muonic atom is 864 ns.

This makes neutrinoless $\mu^- \rightarrow e^-$ conversion very attractive experimentally. Firstly, the e^- energy of about 105 MeV is well above the end-point energy of the muon decay spectrum (~ 52.8 MeV). Secondly, since the event signature is a mono-energetic electron, no coincidence measurement is required. Thirdly, the long lifetime means backgrounds associated with the beam flash can be eliminated. Thus, the search for this process has the potential to improve sensitivity by using a high muon rate without suffering from accidental background events.

4. The COMET experiment

COMET experiment seeks to measure the neutrinoless, coherent transition of a muon to an electron ($\mu \rightarrow e$ conversion) in the field of an aluminum nucleus. The experiment will be carried out using a two-staged approach, Phase-I and Phase-II.

The COMET **Phase-I** aims at a signal sensitivity (SES) of 3.1×10^{-15}, roughly a factor 100 better than the current experimental limit. The goal of the full experiment is a SES of 2.6×10^{-17}, which we refer to as **Phase-II**. This ultimate sensitivity goal is a factor of about 10,000 better than the current experimental limit of $B(\mu^- + Au \rightarrow e^- + Au) \leq 7\times10^{-13}$ from SINDRUM-II at PSI [10]. A schematic layout of the COMET (Phase-I and Phase-II) experiment is shown in Fig.1.

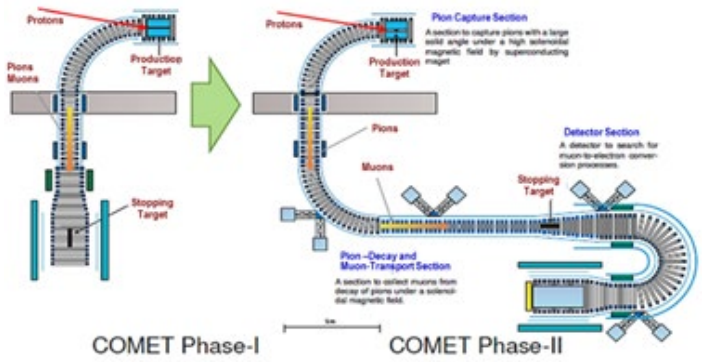

Fig.1 Schematic layout of COMET Phase-I and COMET Phase-II.

The experiment will be carried out in the Nuclear and Particle Physics Experimental Hall (NP Hall) at J-PARC using a bunched 8 GeV pulsed proton beam with high inter-bunch extinction

factor, that is slow-extracted from the J-PARC Main Ring (MR). Muons for the COMET experiment will be generated from the decay of pions produced by collisions of the 8 GeV proton beam on a production target. The yield of low-momentum muons transported to the experimental area is enhanced using a superconducting pion-capture solenoid surrounding the proton target in the pion-capture section. Muons are momentum- and charge-selected using curved superconducting solenoids in the muon-transport section, before being stopped in an aluminum target. The signal electrons from the muon-stopping target are then transported by additional curved solenoids to the main detector system, including a cylindrical drift chamber (CDC), a straw-tube tracker and electron calorimeter, called the StrECAL detector.

4.1 COMET Phase-I

The COMET Phase-I will have the pion-capture and the muon-transport sections up to the end of the first 90° bend of the full experiment. The muons will then be stopped in the aluminum target at the center of a cylindrical drift chamber in a 1T magnetic field. A schematic layout of the COMET Phase-I setup is shown in Fig.2.

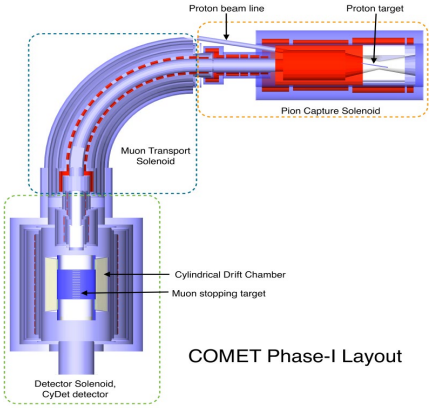

Fig.2 Schematic layout of COMET Phase-I.

The COMET Phase-I experiment will utilize about 3 kW of 8 GeV protons from the J-PARC MR, delivered in pulses spaced by 1.17 μs. For COMET Phase-I, the primary detector for the neutrinoless $\mu-e$ conversion signals consists of a CDC and a set of trigger hodoscope counters, referred to as the CyDet detector. The experimental setup for Phase-I will be augmented with prototypes of the Phase-II StrECAL detector. As well as providing valuable experience with the detectors, the StrECAL and CyDet detectors will be used to characterize the beam and measure backgrounds to ensure that the Phase-II single event sensitivity of 2.6×10^{-17} can be realized [15].

For Phase-I a total number of protons on target (POT) of 3.2×10^{19} is planned which will provide around 1.5×10^{16} muons stopped in the target. This will enable the design goal of COMET Phase-I to be achieved; a single event sensitivity, which, in the absence of a signal, translates to a 90% confidence level branching ratio limit of 7×10^{-15}. This is a factor of about 100 than that of the current limit on gold from SINDRUM-II [10].

4.2 COMET Requirements

In order to obtain the desired improvement in sensitivity, the experiment requires an intense muon source, coming from a pulsed proton beam with high inter-bunch extinction factor.

4.2.1 Highly intense muon source

To achieve an experimental sensitivity better than 10^{-15}, more than 10^{16} muons are needed. To

increase the muon beam intensity, we can use a high-power proton beam from J-PARC, or to use a highly efficient pion collection system, by surrounding the proton target with a 5T superconducting solenoid. The principle of this pion-capture system has been experimentally demonstrated at the MuSIC (Muon Science Innovative beam Channel) facility at Research Centre for Nuclear Physics (RCNP), Osaka University [16].

4.2.2 Proton beam pulsing with high proton extinction

There are several potential sources of electron background events in the signal energy region, one of which is prompt beam-related background events. In order to suppress the occurrence of such background events, a pulsed proton beam will be employed, where proton leakage between the pulses is tightly controlled. As a muon in an aluminum muonic atom has a lifetime of the order of 1 μs, a pulsed beam can be used to eliminate prompt beam background events by performing measurements in a delayed time window, provided that the beam pulses are shorter than this lifetime and the spacing between them is comparable or longer. Stringent requirements on the beam extinction, defined as the number of leakage protons with respect to the number of protons in a beam pulse, are necessary. Tuning of the proton beam in the MR, and using extinction-improving techniques, extinction factor at level 10^{-11} achieved.

4.2.3 Curved solenoids for charge and momentum selection

High momentum muons can produce electron background events in the energy region of 100 MeV, and therefore must be eliminated. This is achieved by transporting the pion/muon beam through a system of curved superconducting solenoids. Hence, with suitably placed collimators, high momentum and positively charged particles can be eliminated. Since the muon momentum dispersion is proportional to a total bending angle, the COMET C-shape beam line produces a larger separation of the muon tracks as a function of momentum and hence an improved momentum selection. In COMET Phase-II, additional curved solenoids will be used in a C-shaped electron transport system between the muon stopping target and the electron spectrometer to eliminate low-momentum backgrounds to the electron signal.

4.3 The Phase-I purpose

The purpose of COMET Phase-I is two-fold. The first is to make **background measurements** for COMET Phase-II and the second is a **search for *μ*−*e* conversion** at an intermediate sensitivity. The COMET Phase-I serves several roles that are highly complementary to the Phase-II experiment. It provides a working experience of many of the components to be used in Phase-II and enables a direct measurement of backgrounds. Significantly, it will also produce competitive physics results, both of the μ−*e* conversion process and of other processes, that COMET Phase-II cannot investigate.

4.3.1 Background measurements

While the signal of $\mu^- N \rightarrow e^- N$ is 105 MeV mono-energetic electron, there are several potential sources of electron background events in the energy region around 100 MeV, which can be grouped into three categories as follows: intrinsic physics backgrounds, which come from muons stopped in the target; beam-related backgrounds, which are caused by both muons and other particles in the muon beam; other miscellaneous backgrounds due to cosmic-rays, fake tracking events etc.

Phase-I will be used to obtain data-driven estimates of backgrounds, and hence inform the detailed design of COMET Phase-II. In Phase-I the StrECAL detector will be placed at the downstream end of the muon-transport beam line and will be dedicated to background measurements, in particular: direct measurement of the inter-bunch extinction factor, direct measurement of unwanted secondary particles in the beam line such as pions, neutrons, antiprotons, photons and electrons, direct measurement of background processes that have not been measured at the required accuracy, such as muon decays in orbit (DIO) and radiative muon capture (RMC).

The total estimated backgrounds for Phase-I is about 0.032 events for a single event sensitivity of 3×10^{-15} with a proton extinction factor of 3×10^{-11}.

4.3.2 Search for μ−e conversion

Even in this partial configuration, COMET Phase-I will conduct a world-leading measurement of *μ−e* conversion using the CyDet detector located inside a 1 T solenoid magnet surrounding the muon-stopping target. This cylindrical geometry is necessary, since the curved electron transport solenoid will not be deployed in Phase-I and thus a planar type detector such as the StrECAL detector would suffer from backgrounds caused by beam related particles.

The CyDet will measure the DIO electron spectrum with a momentum resolution of about 200 keV/c. This measurement can be compared with the theoretical prediction. Once the DIO rate and spectrum are precisely measured, they can be used to monitor the total number of muons stopped in the muon stopping target.

In the COMET Phase-I also we have the radiative muon capture (RMC) at the region of photon energy at the endpoint for aluminum. Again, this measurement cannot be done at an existing muon facility since the number of muons required cannot be obtained. This measurement needs an energy resolution less than 1 MeV since the endpoint is about 3.06 MeV lower than *μ−e* conversion signal. In the COMET Phase-I, the CyDet can be used as a pair spectrometer with a photon converter to measure photon energies of 100 MeV with an energy resolution of about 200 keV.

4.3.3 Other searches

In contrast to COMET Phase-II, the CyDet detector surrounds the muon stopping target directly in Phase-I, and can observe both positive and negative particles from the muon stopping target. This allows for a search for the lepton-number-violating process $\mu^- N \rightarrow e^+ N'$ (μ^--e^+ conversion) concurrently with the $\mu^- N \rightarrow e^- N$ search. The anticipated experimental sensitivity for μ^--e^+ conversion could be similar to $\mu^- N \rightarrow e^- N$ conversion. In addition, the CDC will have a relatively large geometrical coverage, and thereby a coincidence measurement with a large solid angle is achievable. This allows a search for $\mu^- e^- \rightarrow e^- e^-$ conversion in a muonic atom, which is an as-yet unmeasured process. Using a lower intensity beam, < 10^7muon/s, a measurement of $\mu^- e^- \rightarrow e^- e^-$ could be carried out with the CyDet detector.

4.4 Physics Sensitivity for Phase-I

COMET will operate in CyDet mode to search for *μ−e* conversion in Phase-I. The single event sensitivity (SES) is determined for a given number of stopped muons. The SES is given by:

$$B(\mu^- + Al \rightarrow e^- + Al) = \frac{1}{N_\mu \cdot f_{cap} \cdot f_{gnd} \cdot A_{\mu-e}}, \quad (2)$$

where N_μ is the number of muons stopped in the target. The fraction of captured muons to total muons on target f_{cap} = 0.61 is taken, while the fraction of μ−e conversion to the ground state in the final state of f_{gnd} = 0.9 is taken [17]. $A_{\mu\text{-}e}$ = 0.041 is the net signal acceptance. To achieve SES of 3.1×10^{-15}, $N_\mu = 1.5\times10^{16}$ is needed. By using the muon yield per proton of 4.7×10^{-4} a total number of protons on target (POT) of 3.2×10^{19} is needed. With a proton beam current of 0.4 μA, the measurement requires about 150 days although there are considerable uncertainties such as the pion production yield.

5. COMET Phase-*α*

Phase-*α* is planned to be implemented before Phase-I in 2022. In Phase-*α*, we will measure the kinematic parameters for each secondary particle, such as time and energy, as well as the proton beam itself. The yields are roughly 10^{-5} – 10^{-6} times as much as those in Phase-I, due to the limited geometrical acceptance. For PID, we have used a combination of a plastic scintillator hodoscope and the COMET ECAL. We show that e^- and most μ^- are clearly identified, while the PID efficiency for π^-, at less than 80% generally, requires further improvement.

The studies were performed using a fully-detailed geometry. In order to more precisely estimate the secondary beam yield and its characteristics, we will carry out a mass production of simulation data with the newer setup. This will allow us to evaluate the PID performance with more Phase-*α* information. At the same time, the materials and dimensions of the vacuum windows remain to be optimized.

Concerning the PID performance study, some issues require further consideration. First, was not taken into account the effects of particle decays between the two detectors. Second, the positions and dimensions of the detectors need optimization to achieve higher statistics. Third, more variables algorithms should be examined for enhancing the PID performance for π^-. Finally, other possible detector combinations will be explored.

We are also considering the following items, going beyond PID studies. **First**, the ability of Phase-*α* to measure antiprotons is being investigated. Antiprotons are a potential source of backgrounds, but the production cross-section in the backwards direction is not well- understood. If this is measured to be small or cannot be seen in Phase-*α* (in this case we would obtain an upper limit for antiproton production), this would represent an important milestone for the physics measurement in Phase-I. We are now implementing antiproton-producing physics models in our simulation software. **Second**, more concrete studies need to be performed for the PID study, going beyond the basic parameters that have been used above, and incorporating realistic detector effects. **Third**, the detectors for measurements of the proton beam are also being developed at this time. **Fourth**, we plan also to use a target made of aluminum in a setup that will allow us to demonstrate the measurement of muonic X-rays. Lastly, we may install a beam blocker in the detector region and assess its stopping power, because in the Phase-I beam measurement programme, it will be used to suppress the secondary beam flux before it reaches the detectors, and simulation work will be needed to optimize the design of this component.

6. JINR contribution

The main contribution of JINR to COMET consists of participation in the production of three main detector systems: the electromagnetic calorimeter, the straw tracker, the Cosmic Ray Veto System, and variety of works on simulation.

6.1 R&D of LYSO crystals

For calorimeter, we performed R&D of LYSO crystals used for ECAL cells. The losses of the light yield along the crystal length, non-uniformity, energy resolution were experimentally measured. For this research LYSO crystals (20×20×120 mm^3), doped with 1.5% cerium of Saint-Gobain production, were used. In addition, a comparative estimate of the light yield for these crystals was obtained. The studies were performed by using a precision measuring setup, the results are published in [18], [19]. It is established, that the energy resolution (FWHM) is on average equal to 8.9%, the coefficient of the non-uniformity is about 1.2 %/cm^{-1}.

The non-uniformity of the light yield along the crystal length affects the accuracy of the measurement of the energy released in the calorimeter. In order to reduce the non-uniformity of the light yield, it is necessary to ensure a uniform collection of photons along the crystal length of the crystal. To reduce these losses, special light-reflective wraps are used. For the development of techniques to improve the light collection we have investigated the light yield non-uniformity and energy resolution along the crystal length. It was obtained that improvement of light collection could be achieved by use TEFLON tape as the diffusion-type layer (inner layer) and ESR as mirror type layer (outer layer) [20], [21], [22].

In addition, an experimental study of the angular error of the released energy measurement in crystals on the Dubna prototype was performed using a ^{60}Co source. It was obtained, that the error in measuring the released energy on cosmic muons for an angle of 20 degrees is ~ 6.7%, which is consistent with the results of measurements of the prototype calorimeter on an electron accelerator (Beam Test 2014, Tohoku, Japan) [19].

The optical parameters (energy resolution, decay time, relative light yield, non-uniformity of the light distribution along the length) of a new (engineering) LYSO crystal from Saint-Gobain was made. It was obtained, that the light output of the LYSO engineering crystal is approximately 20% greater than previously produced crystals, but the energy resolution is practically the same, decay time is slightly shorter, the standard deviations of the light yield along the crystal length for a group of 10 samples relative to their average value compose about 10% to 19%.

The optical parameters (energy resolution, decay time, relative light yield, non-uniformity of the light distribution along the length) of the Chinese crystal by JT Crystal Technology Co. Ltd. (as a possible candidate) are studied in detail. The non-uniformity of the scintillation properties: light yield and energy resolution of LYSO crystals by Saint-Gobain (France) and JT Technology Co. Ltd. (China) were investigated by gamma and optical spectroscopy methods [23]. Comparison of the optical properties of the two crystals allows us to conclude that the Saint-Gobain crystals have a more uniform distribution of the scintillation properties, and that they have fewer optical traps and crystal structure defects.

6.1.1 LYSO crystals certification

The purpose of certification of the crystals LYSO(Ce) is to obtain the individual properties of each crystal. The measured properties are the relative light output, the attenuation of light in the crystal, and the non-uniformity of the light output. For these measurements, a stand was created. Modernization and maintenance of the stand was carried out.

The measurements were carried out using a radioactive source Na-22. For each crystal, we get a passport describing its main characteristics. Currently, more than 250 crystals are measured, 200 passports are prepared.

6.2 Straw-tube R&D and production at DLNP, JINR

Over the past years, a method of using ultrasonic welding technologies of straw production, which does not require multiple over-woven layers, has been developed by the JINR group for the NA62 experiment at CERN [24]. In this method, a single layer is rolled and attached to itself in a straight line without using glue. Later by JINR-COMET group, this method and equipment were obtained in order to be improved and 2700 units of straw tubes were made for Phase-I with thinner wall 20 μm and 9.8 mm in diameter. Many stress and long-term holding tests showed their reliability for using in vacuum conditions.

At this moment an active modules assembly for Phase-I is in progress at J-PARC, our participation in this is still difficult due to the pandemic, but we hope to be involved strongly soon.

According to the main requirements of COMET project in Phase-II there must be used straw tubes with 12 μm thick walls and 5 mm in diameter. Thin walls of straw tubes were being a crucial moment for tracker detector in order to reduce multiple scattering. In order to achieve the mentioned goals and make straws with the required parameters, the JINR-COMET group created a special laboratory (Clean Room) to develop and produce unique straw tubes with new parameters using ultrasonic welding technology. For ensuring of getting steady parameters for straw in the “clean room” follow conditions have been controlled**:** air cleanness grade in 6 class (particles with dimension ≤5 micrometer should be less than 20000 per 1 m^3); temperature with accuracy ±0.1^oC; humidity ±5%. After configuring the welding machine and the first studies, the first welded pipes of straw with a length of 1400 mm, a thickness of 12 μm and a diameter of 5-10 mm were obtained, Figure 3.

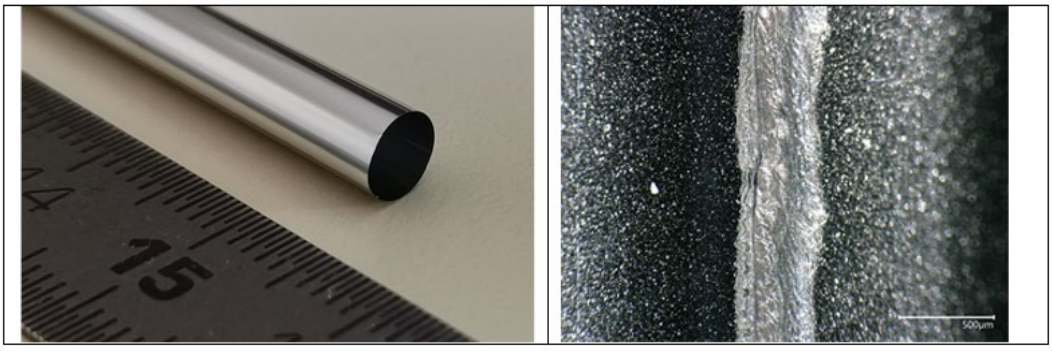

Fig.3 12 μm straw tube and welded seam structure.

The quality of the seam (shown at Fig.3), was checked and showed good results for the preliminary tests. Straw tubes were pressurized on a working pressure 1 bar and after that pumped up with argon to 3 bar. The tubes held pressure without any leakage and visible damages. The other stress tests of 12 μm straw tubes and seam characteristics showed excellent results for quality and reliability.

In the future, a more thorough study of the properties of straw tubes and the development of tests for quality control is planned**:** for carrying out full scale tests for new 5mm straw tubes we start manufacture prototype, which consist of four layers with 16 straws in which layer. Length of tubes is 500mm. For tube assembling the very important details engineering development is carried out**:** micro-pins and end-plugs. Test experiment should be done on electron beams of Laboratory Nuclear Problems accelerator.

With the help of the stand created for diameter scanning (Figure 4), a 5mm tubes scans with different pressure levels have been performed.

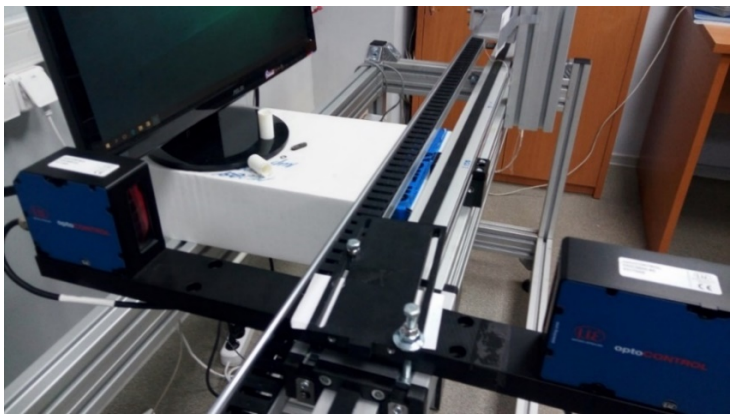

Fig.4 Stand for tube scan.

It is important that taking into account the success of JINR DLNP COMET group in R&D and production of thin-wall tubes with 5 mm diameters, and development of straw station design, the COMET collaboration supports the idea of JINR group to use an additional station with new tubes at Phase-I, Figure 5.

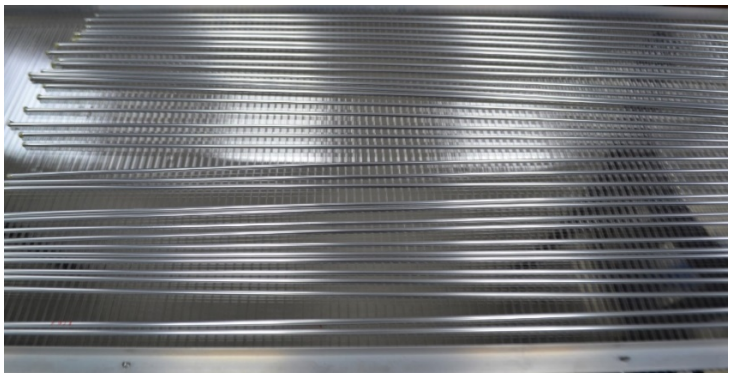

Fig.5 New type straw tubes.

After the completion of all research work, the mass production of the COMET Phase-II experiment will begin.

6.2.1 Straw tubes testing in KEK, J-PARC

Within the Phase-I 2700 full-size (1.2 m and 1.6 m length) straw tubes have been produced, after testing and checking according to quality standard all tubes were sent to Japan at KEK and from there to J-PARC. Due to the specific properties of Mylar and 20 μm wall thickness of straw tubes, long-term keeping requires constant monitoring and controlling of storage condition (quality control procedures must be carried out every 6 months). Experience has shown that in order to maintain normal physical storage conditions and ensure safe transportation from JINR to the KEK, the tubes must be under pressure. This also makes it possible to observe their behavior under similar conditions, like in a detector. For this, the tubes were prepared with the following conditions: initial gas pressure ~2.5 bar. At the J-PARC started a regular checking process of the straw tube conditions. By results, the pressure in the tubes dropped about 0.7 bar during 2 years of storage. This is an excellent result for 20 μm wall thickness straw tubes. One of the causes of gas leakage is micro-shells between the wall of the straw and the endplugs, as well as the rubber ring between the endplugs and the gas blockers. In conclusion, the first measurements were done successfully, all safety conditions for long-term keeping are restored and straw tubes are ready for assembling in detector modules and for afterward tests.

6.2.2 Study of the properties of straws

In order to ensure straw detector's high coordinate accuracy, in addition to the precise positioning of the wire inside the tube and the tubes themselves in the detector's modules the material from which straws are made is required to maintain its basic physical properties over time. As well as the material is required to be uniform throughout the length of the tube. The most important straw material's physical properties are: the area of elastic deformation, the value of the elastic modulus, which characterizes the straw strength depends, the relaxation rate of tension. The Poisson's ratio allows determining the impact of pressure drop on the straw wall on its tension. These parameters largely influence the detector design's choice and the straw lifetime in the experiment. We defined working parameter space for our 9.8 mm straws. The results of measurements were prepared for publication. A patent was also obtained for the invention on the bench with thermo-stabilization system for measuring of properties of the straws.

For the COMET-Phase II straw detector there will be used straw tubes 4.8 mm, which imposes severe restrictions on the quality of mass production of straw. For these purposes, a test bench was developed and built that allows to evaluate dependence of the tube diameter on internal pressure and dependence of tube diameter on tension, also evaluate the contribution of internal pressure to tube tension.

6.3 Straw-ECAL combine test beam

Straw-ECAL combine test-beam experiment was conducted at ELPH (Research Center for Electron Photon Science, Tohoku University, Japan), on an electron (1.3 GeV) beam with the participation of members of the COMET collaboration from the DLNP JINR. On the 105 MeV beam with spot size $\sigma_x \sim 6$ mm and $\sigma_y \sim 3$ mm were tested prototypes of an electromagnetic calorimeter and a straw tracker. A calorimeter prototype was composed of 16 modules of LYSO crystals. Each module consisted of four crystals; in total in the prototype were 64 crystals. The crystals used in test-beam have been thoroughly investigated in DLNP JINR [19] first, including light yield, light absorption, homogeneity etc. For beam test was prepared and assembled in KEK by KEK-JINR groups full-size straw tracker prototype, using straw tubes developed and produced by JINR group. The 20-μm wall-thickness straws are mounted using the newly-developed feedthrough system and the entirety of the exterior is covered with a vacuum wall so that it can be evacuated, allowing the behavior in vacuum to be investigated. The prototype is constructed of aluminum so that it will not be affected by magnetic fields. Straw tubes showed closed to 100% efficiency for the Ar:C_2H_6 (50:50) gas mixture starting 1800 V applied HV. A spatial resolution of 143.2 μm for the HV of 1900 V is obtained. This value includes the uncertainties arising from the precision of track reconstruction, and if this is taken into account the true spatial resolution is estimated to be 119.3 μm. For 105 MeV electron energy resolution for the calorimeter prototype varies from 3.8% to 4.4%, depending on the beam hit, the position resolution is $\sigma_R = 5.8$ mm. In conclusion, Straw-ECAL combine test results, are confirmed to meet requirements.

6.3 Cosmic-Ray Veto (CRV)

Muons from cosmic rays mimic the 105 MeV conversion electrons and, as a major source of background, would reduce the experiment overall precision. So, to suppress the cosmic muons, the Cosmic-Ray Veto (CRV) system becomes as an essential part of the COMET experiment. It will cover around of the COMET other systems and will acting as an active shielding and efficiency to record the muon is required on 99.99% level.

CRV will consist of two major parts: scintillator based (SCRV) and GRP chambers based (BS-CRV) subsystems. The SCRV subsystem placed on top, sides and back of the COMET and based on extruded plastic scintillation strip with WLS fiber glued to the strip groove. The BS-CRV will be placed in hottest area at front of the COMET and will be consists of array of GRPC.

The JINR group is the leader in R&D, in design and in development of the SCRV subsystem. This activity includes two parts: to finalize design of the SCRV with providing scintillation strips production, testing, CRV modules creation schedule and to design/create/test the electronics embedded to the scintillators.

Last year, we did some R&D searches with such design (including the simulation and experimental results for 4x4 module) and was found that the design of SCRV based on 4-layers array of plastic scintillator strips 7x40 mm^2 in cross section and with one 1.2-mm in diameter Wave-Length Shifting (WLS) optical fiber glued in the groove along the strip will not be able to provide necessary 99.99% efficiency for muon registration.

Based on JINR teams' searches and including the aging (deterioration of the light yield by time) effect, we proposed different configurations for strips: with one or two WLS fiber in parallel grooves, with different WLS fibers diameters, combination of it. Also, we continue to find the best values for the shift layer to each other (so called pattern) and plan to test it in test 4x4 module. Was found that configuration of 7-mm thick strip with two 1.2-mm WLS fibers and SIPM with 3x3 mm^2 active area have the best ration of efficiency to cost ratio, but the best configuration is 10-mm with two 1.4 WLS fibers. Both configurations are the subject of discussions.

The final design of the strip will be discussed during the COMET Collaboration Meeting and once it approved, we will create the so-called "Module-0" and start strips mass production.

Other activity of the JINR team is to create the embedded and front electronic for SCRV based on CITIROC family chipset as of the best solution by the ratio of the quality/cost/electricity consumption. The first prototype with 32 channels based on CITIROC will be ready for test by the spring of 2021. This FEBE will be attached to the short prototype of the 4x16 module (already created) to test its properties. Special flexible PCB, which should hold the SiPM on the end and connected to FEBE with other, already designed. Special mezzanine PCB board will ensure that all SiPM is attached properly to the strips.

It is important to test the SCRV prototype readout attached in high radiation environment with neutron flux close to the predicted by simulation level of 10^{+9} neutron per cm^2. It is possible to be done in IBR-2 facility at JINR. The deterioration of light yield for SCRV prototype under such flux should be learned as well as stability of the FEBE prototype under such radiation.

7. The responsibility of the JINR in the COMET

- The JINR group is a single one in the COMET collaboration, which is capable to produce thin-wall straw tubes. Therefore, we are **fully responsible** for manufacturing of all straw tubes. Different procedures of the tube tests on pressure, gas leakage and elongation have been also updated in accordance with the COMET requirements and new test standards have been established.
- JINR takes **full responsibility** for the next step to this direction, carrying out of R&D works of straw tubes for the COMET Phase-II, with the tubes of 5 mm diameter and 12μ wall thickness. For this purpose, we are preparing a new straw line in DLNP.
- JINR physicists together with the KEK colleagues take **full responsibility** in assembling, tests and installation of the full-scale straw tracker for Phase-I. Appreciating the crucial contribution

of the JINR to the creation of the straw tracker, a member of JINR-COMET team was elected as one of the **coordinator for the straw tracker system.**

- JINR proposed the idea and takes **full responsibility** in production of a full-scale straw station for Phase-I, with new type of straw tubes.
- JINR takes **full responsibility** for development and optimization of a crystal calibration method for the calorimeter to be used in COMET Phase I and Phase-II.
- JINR together with KEK and Kyushu University takes **full responsibility** for assembling, testing, installation and operation of the calorimeter.
- Physicists from JINR take **full responsibility** for the certification of crystals, and are the leaders in the R&D work.
- JINR physicists have implemented a full-scale R&D program to create a cosmic veto system. The program was completed successfully, and the results were reported at the collaboration meetings. Based on these results, all the parameters and methods for creating the CRV are determined. Also, the **main responsibility** in the assembly, testing and installation of the CRV for Phase-I will be on scientists from JINR. Based on these, a member from JINR group was elected as the COMET-CRV leader.

8. Further plans foresee

- Participation in the preparation, engineering and physics run, the data acquisition and analysis of Phase-*α*, 2022-2023
- Finalization assembling, testing, calibration, installation, cosmic test and maintenance of the straw detector for Phase-I, 2022-2023
- R&D program for production of the straw tubes of 12 μm wall thickness and 5 mm diameter. Measuring of all mechanical properties and development of standards for quality control of manufactured of the 5 mm brand-new straw tubes, 2022 -2023
- Creating a straw prototype (64 channels) with new tubes (12 μm, 5 mm) and measurement on the beam, 2022-2023
- Production of straw tubes (about 1000 pcs) for full-scale prototype, 2022
- Production of a full-scale straw station for Phase-I, with new tubes (12 μm, 5 mm), and measurements on the beam, 2022-2024
- Preparation for mass-production and testing of straw tubes for Phase-II, 2024
- Test (certification) of the LYSO crystals, to be used in the calorimeter, 2022-2023
- Development and optimization of a crystal calibration method for a COMET calorimeter, given the features of the experiment: the presence of a magnetic field and high resolution calorimeter**,** 2022-2023
- Participation in the calorimeter designing, assembling, installation, cosmic test and maintenance**,** 2022-2023
- Participation in the assemble and maintenance of the CRV for Phase-I, 2022-2023
- Participation in assembling, testing, installation and maintenance of whole detector system for Phase-I, 2022-2023
- Complex detector system (tracker, calorimeter, etc.) simulation, 2022-2024
- Participation in the engineering and physics run**,** 2023-2024
- Participation in the data acquisition and analysis, 2023-2024
- Participation in the beam tests of the detector components for Phase II, 2023-2024

9. Summary and Prospect

- The implementation of Phase-α is an important step for Phase-I. It will give us the opportunity to understand the 8 GeV proton beam transported to the COMET experimental area and π/μ production yield in the backward direction at 8 GeV without the Pion Capture Solenoid (PCS). This enables us to measure the proton beam characteristics, extinction factor and π/μ production. The secondary particles produced at the graphite target in the backward direction will enter to the TS and are transported to the detector region of the COMET experimental area. Phase-α will demonstrate muon transport via TS to the COMET experimental area. Secondary-beam measuring detectors will be set in the COMET experimental area and measure the beam phase space with possible particle-identification (PID).
- The first stage of the COMET programme will provide an opportunity to fully understand the novel superconducting pion production system and muon beam line, with its charge-and-momentum selecting dipole fields which are superimposed on the curved solenoids which form the pion and muon transport section - a design that is unique to COMET amongst intense pulsed muon beam facilities.
- The research programme for Phase-I encompasses both a search for muon-to-electron conversion with a sensitivity that is about 100 times better than the current limit, and a dedicated detector set-up, which will allow us to make comprehensive measurements of the muon beam.
- Detailed rate and timing studies and other measurements from Phase-I will help us understand the backgrounds to the $\mu \rightarrow e$ conversion measurement. These will be crucial as COMET prepares to move to Phase-II, which is to improve the sensitivity by another two orders of magnitude.
- The challenges to building and running this high-background rare-decay search experiment are addressed, including: proton and muon beam dynamics; the superconducting magnet systems; high-rate data-acquisition systems; operation in harsh radiation environments; software and computing systems that can meet the demands of the experiment.
- The COMET Collaboration believes that rapid execution of Phase-I, which will consist of data taking in numerous different configurations of the beam line and detector systems, to be followed by the deployment of Phase-II soon after, is the most reliable path to a high-sensitivity search for $\mu \rightarrow e$ conversion. The programme has the potential to result in a paradigm-shifting discovery, which could lead to an entirely new field opening up of multiple measurements of different charged-lepton flavour violating processes - a new era of discovery in particle physics.
- The important role of JINR in the COMET experiment is quite visible and highly recognized by the COMET Collaboration.

10. Estimation of human resources

COMET JINR group members (bold – new members)

#	Name	FTE	Position	Work (apart common duties like shifts)
1	**G. Adamov**	0.7	Junior researcher PhD student	Hardware and Software tools development, data quality control, analysis
2	**A.M.Artikov**	0.5	Senior scientist	Hardware development and support of CRV
3	D. Aznabayev	0.3	Junior researcher	Theoretical issues, physics analysis
4	D. Baygarashev	0.4	Junior researcher	Data quality control, calibration, physics analysis
5	**A. Boikov**	0.3	Junior researcher PhD student	CRV electronics, R&D COMET
6	**D. Chokheli**	1.0	Senior scientist	CRV construction, Leader of COMET-CRV detector system
7	V.N. Duginov	0.8	Deputy head of department	Calorimeter development, analysis
8	T.L. Enik	0.3	Senior scientist	Hardware development and support
9	I.L. Evtoukhovitch	0.9	Senior engineer	Hardware development and support
10	D. Goderidze	0.5	Junior researcher PhD student	Software/analysis
11	P.G. Evtoukhovitch	1.0	Senior scientist	Coordinator of Straw Tracker detector system
12	A. Issadykov	0.3	Senior scientist	Theoretical issues, physics analysis
13	V.A. Kalinnikov	1.0	Leading scientist	Calorimeter development, MC, analysis
14	E.S. Kaneva	1.0	Engineer	Hardware/software
15	X. Khubashvili	0.9	Engineer	Hardware development and support
16	A. Khvedelidze	0.4	Leading scientist	Theoretical issues, models development
17	**A. Kobey**	0.5	Master student	Calorimeter development, MC, analysis
18	G.A. Kozlov	0.3	Leading scientist	Theoretical issues, models development
19	A.S. Moiseenko	1.0	Scientist	Hardware development and support
20	A.V. Pavlov	1.0	Junior researcher PhD student	MC, Data quality control, physics analysis
21	B.M. Sabirov	1.0	Scientist	Hardware development and support
22	A.G. Samartsev	0.4	Senior engineer	Hardware development, detector design
23	**A.V. Simonenko**	1.0	Senior scientist	CRV creation and maintenance
24	**V.V. Tereschenko**	0.3	Head of group	CRV electronics, R&D COMET
25	**S.V. Tereschenko**	0.5	Engineer	CRV electronics, R&D COMET
26	Z. Tsamalaidze	0.8	Head of sector	Leader of COMET-JINR group, IB represent.
27	N. Tsverava	1.0	Junior researcher PhD student	Hardware development, calibration, analysis
28	**I.I. Vasilyev**	0.3	Junior researcher	Calorimeter R&D and tests
29	E.P. Velicheva	1.0	Senior scientist	Calorimeter development, MC, analysis
30	A.D. Volkov	1.0	Scientist	Hardware development
31	**I. Zimin**	0.5	Junior scientist PhD student	Software, simulation, analysis
	Total FTE	**20.9**		

The average age of the JINR COMET team is ~ 44 years, including 1 master and 9 junior researchers.

11. Concise justification of the requested expenditures

During the entire extension period of the project, we plan to maintain and develop the above-mentioned results of the JINR group's activity in COMET. In addition, we must fulfill the

responsibility that the collaboration has imposed on us. Especially it should be noted the full responsibility for production of a full-scale straw station for Phase-I, and creating of the CRV system.

The following resources are requested for the proposed extension of the COMET project at JINR for the period of 2022-2024:

1. 330K$ (190 + 140) - Materials and Equipment's for:
   - R&D and construction of CRV modules (scintillation strips, SiPM, fibers and other components),
   - the straw tubes R&D, straw tubes production and full-scale prototype creation (Maylar for straw tubes production, equipment for straw tube stand, optical sensors, pressure sensors, printing plastic for the 3D, other components),
   - R&D and construction of ECAL (PMT's, wrapping material, sources, other components),
   - computers: personal computers and servers for software development and simulation and data analysis.
2. 300K$ - Money for:
   - visiting the COMET collaborating laboratories in KEK and J-PARC,
   - participating in conferences and meetings.
3. 60K$ - Research operation fee.

12. SWOT (Strengths, Weaknesses, Opportunities and Threats) Analysis

The JINR scientists fruitfully participated in the COMET experiment since the very beginning of the experiment. The history of research in muon physics comes from the DLNP early times.

The strength of the Project is to participate on the front end of particle physics and New physics searches in the CLFV sector which is widely recognized by world community and is complimentary to new model tests at LHC. In practice, this Project brings together JINR employees' participation in the world's main experiment to search for CLFV processes with muons on the energy scale in the search for new physics. JINR colleagues have achieved great success in preparing for the operation of the respective detectors. In particular, we created a stand and conducted the first tests on welding of ultrathin 12 microns straw tubes. Employees of DLNP implemented a serious R&D program for new type of LYSO crystals and proposed a way to increase the light collection from LYSO crystals for electromagnetic calorimeter.

It should also be noted about the serious strengthening of the COMET JINR team, and in general the collaborations also by adding experts of CRV, which gave us the opportunity to make a crucial contribution for the CRV R&D, and in the near future to the creation of CRV, which is very welcome by Japanese colleagues. Also, the strengthening of the team accordingly increases the activity of the JINR's group in software (simulation and future data analysis).

Now the activity of the JINR's group covers all three main directions (straw tracker, calorimeter and the CRV) of the detector system. Therefore, JINR became one of the leaders of the COMET collaboration.

The relatively weakness in the current situation is that, according to the PAC recommendation, first of all we should implement Phase-alpha, and then Phase-I, which will slightly change the implementation time of the COMET Phase-I experiment.

13. References

1. COMET Phase-I TDR, COMET Collaboration, PTEP 2020, 3, 033C01.
2. The COMET Collaboration, *Conceptual design report for experimental search for lepton flavor violating $\mu^- \rightarrow e^-$ conversion at a sensitivity of* 10^{-16} *with a slow-extracted bunched proton beam (COMET)*, KEK Report 2009–10 (submitted to the J-PARC Physics Advisory Committee) (2009). https://lib-extopc.kek.jp/preprints/PDF/2009/0924/0924011.pdf
3. L. Bartoszek, et al. (Mu2e Collaboration), arXiv: 1501.05241 (2015).
4. S.T. Petcov, Sov. J. Nucl. Phys. 25 (1977) 340.
5. L. Calibbi and G. Signorelli, Riv. Nuovo. Cimento, 41 (2018) 71.
6. V. Cirigliano, et al., Phys. Rev. D80 (2009) 013002.
7. E.P. Hincks and B. Pontecorvo: Search for Gamma-Radiation in the 2.2-Microsecond Meson Decay Process. Phys. Rev. 73 (1948) 257. https://doi.org/10.1103/PhysRev.73.257
8. A. Baldini, et al. (MEG Collaboration), Eur. Phys. J. C76 (2016) 434.
9. U. Bellgardt, et al. (SINDRUM Collaboration), Nucl. Phys. B299 (1988) 1.
10. W. Bertl, et al. (SINDRUM-II Collaboration), Eur. Phys. J. C47 (2006) 337.
11. T. Hambye, Proc. Nucl. Phys. B248 (2014) 13.
12. A. Abada, et al., JHEP 11 (2014) 048.
13. J. Kaulard, et al. (SINDRUM-II Collaboration), Phys. Lett. B422 (1998) 334.
14. B. Yeo, Y. Kuno, M. Lee and K. Zuber, Phys.Rev. D96, no. 7 (2017) 075027.
15. B. Krikler. “Sensitivity and Background Estimates for Phase-II of the COMET Experiment.” 2016. URL http://hdl.handle.net/10044/1/45365
16. D. Tomono, et al. “Construction of new DC muon beamline, MuSIC-RCNP, for muon applied science.” PoS, NuFact2017:111, 2018. doi:10.22323/1.295.0111.
17. E. Oset, H. C. Chiang, T. S. Kosmas, A. Faessler, J. D. Vergados. “Coherent and incoherent (μ−,e−) conversion in nuclei and background from μ− decay in orbit.” In “13th International Conference on Particles and Nuclei (PANIC 93) Perugia, Italy, June 28-July 2, 1993,” pp. 271-272. 1993.
18. V. Kalinnikov, E. Velicheva. Investigation of LYSO and GSO crystals and simulation of the calorimeter for COMET experiment. // Phys. Part. Nucl. Lett. 11 (2014) 3, 259-268.
19. V. Kalinnikov, E. Velicheva. Research of the ECAL calorimeter used in the COMET experiment. // Functional Materials, 22 (2015), 1, 116-125.
20. V. Kalinnikov, E. Velicheva, Z. Tsamalaidze, Lobko, O. Missevitch, Y. Kuno. Spatial and temporal evolution of scintillation light in LYSO electromagnetic calorimeter for non-paraxial electromagnetic showers. //Nonlinear Phenomena in Complex. V. 19, No 4 (2016). Pp. 345 – 357.
21. В. Калинников, Е. Величева, А. Лобко. Исследование длинных кристаллов GSO и LYSO для создания сегментированных электромагнитных калориметров. Физика сцинтилляторов. Материалы, методы, аппаратура. Изд: ИСМА . 2015. С. 137-158.
22. Калинников В. Величева Е. Исследование параметров и разработка алгоритма пространственной реконструкции для калориметра COMET эксперимента. Изд:ИСМА . 2015. С. 186-203.
23. Kalinnikov et. al, Investigation of the light yield distribution in LYSO crystal by the optical spectroscopy method for the electromagnetic calorimeter of the COMET experiment // Nonlinear Phenomena in Complex Systems, vol. 23, no. 4 (2020), pp. 374 – 385.
24. S. Movchan. Nucl. Instr. and Meth., A604:307, 2009.
25. V. Kalinnikov, E. Velicheva. Simulation of Long GSO Crystals for the COMET Experiment. // Nonlinear Phenomena in Complex. V. 8, No 2 (2015). Pp. 215 – 221.

14. The publications and conferences talks, given by JINR team

Publications

1. V. Kalinnikov, E. Velicheva. Investigation of LYSO and GSO crystals and simulation of the calorimeter for COMET experiment. // Phys. Part. Nucl. Lett. 11 (2014) 3, 259-268.
2. V. Kalinnikov, E. Velicheva. Research of the ECAL calorimeter used in the COMET experiment. // Functional Materials, 22 (2015), 1, 116-125.
3. V. Kalinnikov, E. Velicheva. Research of long GSO and LYSO crystals used in the calorimeter developed for the COMET experiment. Functional Materials, 22 (2015), 1, 126-134.
4. V. Kalinnikov, E. Velicheva. Simulation of Long GSO Crystals for the COMET Experiment. // Nonlinear Phenomena in Complex. V. 8, No 2 (2015). Pp. 215 – 221.
5. В. Калинников, Е. Величева, А. Лобко. Исследование длинных кристаллов GSO и LYSO для создания сегментированных электромагнитных калориметров. Физика сцинтилляторов. Материалы, методы, аппаратура. Изд: ИСМА. 2015. С. 137-158.
6. Калинников В. Величева Е. Исследование параметров и разработка алгоритма пространственной реконструкции для калориметра COMET эксперимента. Изд: ИСМА. 2015. С. 186-203.
7. V. Kalinnikov, E. Velicheva, Z. Tsamalaidze, Lobko, O. Missevitch, Y. Kuno. Spatial and temporal evolution of scintillation light in LYSO electromagnetic calorimeter for non-paraxial electromagnetic showers. //Nonlinear Phenomena in Complex. V. 19, No 4 (2016). Pp. 345 – 357.
8. Kalinnikov et. al, Investigation of the light yield distribution in LYSO crystal by the optical spectroscopy method for the electromagnetic calorimeter of the COMET experiment // Nonlinear Phenomena in Complex Systems, vol. 23, no. 4 (2020), pp. 374 – 385.
9. M. Eliashvili, A. Khvedelidzre, M. Nioradze, Z. Tsamalaidze. The COMET experiment at J-PARC: A step towards solving the muon enigma, TSU Science, N6, (2014).
10. V. Kalinnikov, E. Velicheva. Simulation of Long GSO Crystals for the COMET Experiment. Nonlinear phenometa in complex systems, 18, №2, 215 (2015).
11. А.Д. Волков. Контроль натяжения трубок в строу детекторах. Успехи прикладной физики, 2, №4, 413 (2014).
12. A.D. Volkov. Wire tension monitor for proportional chambers of the ANKE spectrometer. NIM A 701, 80 (2013).
13. А. Д. Волков, М. Д. Кравченко, А. В. Павлов. Стенд для исследования характеристик строу. Успехи прикладной физики, 2019, том 7, № 1, стр. 76 - 83.
14. А. Д. Волков, П. Г. Евтухович, А. С. Моисеенко, Б. М. Сабиров, З. Цамалаидзе, Н. Цверава. Влияние внутреннего давления на натяжение в сварных строу трекового детектора. Успехи прикладной физики, 2018, том 6, № 1, стр. 83 – 90.
15. A. D. Volkov, M. D. Kravchenko ∗, A. V. Pavlov. The test bench for studying the characteristics of straw tubes. JINR Preprint E13-2018-70.
16. A. Volkov*, P. Evtoukhovich, M. Kravchenko, Y. Kuno, S. Mihara, H. Nishiguchi, A. Pavlov, Z. Tsamalaidze. Properties of straw 1 tubes for the tracking detector of the COMET experiment. Accepted in NIM.

17. А.Д. Волков. Устройство для измерения натяжения трубки в строу детекторах. Патент №2539107 (2013).
18. А. Д. Волков, З. Цамалаидзе. Способ определения коэффициента Пуассона материала герметичной тонкостенной полимерной трубки. Патент № 2653186.
19. А. Д. Волков, М. Д. Кравченко, А. В. Павлов. Устройство для исследования свойств строу трубки координатного детектора частиц. Патент № 2691770.
20. COMET Phase-I. Technical Design Report 2016 (prepared with participation of the JINR physicists).
21. H. Nishiguchi, P. Evtoukhovitch, A. Moiseenko, Z. Tsamalaidze, N. Tsverava, A. Volkov, et al. Development of an extremely thin-wall straw tracker operational in vacuum- The COMET straw tracker system. NIM, A 845, 269 (2017).
22. H. Nishiguchi, P. Evtoukhovitch, Y. Fujii, E. Hamada, N. Kamei, S. Mihara, A. Moiseenko, K. Noguchi, K. Oishi, J. Suzuki, J. Tojo, Z. Tsamalaidze, N. Tsverava, K. Ueno, A. Volkov, Construction on vacuum-compatible straw tracker for COMET Phase-I. NIM, A 958 (2020) 162800.
23. A. Artikov, V. Baranov, A. Boikov, D. Chokheli, Yu.I. Davydov,V. Glagolev, A. Simonenko, Z. Tsamalaidze, I. Vasilyev, I. Zimin. High efficiency muon registration system based on scintillator strips, (in preparation for NIM).

Conference talks

1. Z. Tsamalaidze. “The status and plans of JINR activity in the COMET experiment”, the COMET CM22 workshop, Tokai, 29 May – 02 June, 2017
2. A. Pavlov, P. Evtoukhovitch. “Position Resolution of the Straw Tube”, CM23 workshop, TU-Dresden, 24-30 Sep, 2017
3. K. Ueno, P. Evtoukhovitch, et al., “Development of a thin-wall straw-tube tracker for COMET experiment”, Proceedings, 2017 European Physical Society Conference on High Energy Physics (EPS-HEP 2017): Venice, Italy, July 5-12, 2017
4. P.Evtoukhovitch. “Present status of the straw module prototype with 5 mm straws”, CM25 workshop, Tokai, 21-25 May, 2018
5. A. Pavlov. “The effect of the gap on the collection of primary ionization”, CM25 workshop, Tokai, 21-25 May, 2018
6. A. Pavlov. “The effect of the seam on the collection of primary ionization”, European School of High-Energy Physics, Maratea, Italy, 20 June – 3 July, 2018
7. V. Duginov. “The pasportization of the LYSO(Ce) crystals for COMET”, the COMET CM26 workshop, Tbilisi, 1-5 October 2018
8. A. Pavlov. “Simulation of drift lines. The nature of the electron motion in the tube”, CM26 workshop, Tbilisi, 1-5 Oct, 2018
9. M. Kravchenko, A. Pavlov. “Mechanical properties of the thin-walled welded straws for the COMET experiment”, CM26 workshop, Tbilisi, 1-5 Oct, 2018
10. A. Pavlov. “The first step in obtaining a three-dimensional drift line”, CM27 workshop, Tokai, 19-23 Feb, 2019
11. A. Pavlov., P. Evtoukhovitch. “The simplify model of electron drifting in the straw tube”, CM27 workshop, Tokai, 19-23 Feb, 2019

12. P. Evtoukhovitch. “New steps in the straw module development for 5 mm straws”, CM27 workshop, Tokai, 19-23 Feb, 2019
13. A. Pavlov, P. Evtoukhovitch. “The final result of simulation of the drift line in Garfield ++”, CM28 workshop, Tokai, 19-23 Feb, 2019
14. M. Kravchenko. “Mechanical properties of the thin-walled straws of the COMET experiment”, The EPS-HEP2019 Conference, Ghent, Belgium, 10-17 July, 2019
15. N. Tsverava et al., “Development of Ultrathin 12 μm Thick Straw Tubes for the Tracking Detector of COMET Experiment”, Proceedings, 2019 IEEE Nuclear Science Symposium (NSS) and Medical Imaging Conference (MIC) (NSS/MIC 2019): Manchester, United Kingdom, October 26- November 02, 2019
16. H. Nishiguchi, P. Evtoukhovitch, et al., “Construction on vacuum-compatible straw tracker for COMET Phase-I”, The 15th Vienna Conference on Instrumentation, Vienna, Austria, February 18-22, 2019
17. V. Duginov. “The certification of the LYSO(Ce) crystals for COMET calorimeter”, The COMET colloquium, Dubna, October 2019
18. N. Tsverava. “Straw tubes R&D for Phase-II”, CM28 workshop, Tokai, 10-14 June, 2019
19. N. Tsverava. “Examination the quality of the seams of 12/20 μm straw tubes”, CM29 workshop, Tokai, J-PARC, 14-18 Oct, 2019
20. D. Chokheli. “ High Efficiency Muon Registration System based on Scintillator Strips”, CM32 workshop, Tokai, 2-6 November, 2020
21. S. Tereshchenko. “ Proposal for Improvement of the efficiency and electronic for the CRV”, CM32 workshop, Tokai, J-PARC, 2-6 November, 2020
22. D. Chokheli. “ R&D for CRV system based on scintillator strips for the COMET experiment”, CM33 workshop, Tokai, J-PARC, 22 February to 4 March, 2021.

15. Estimation of costs and resources

Form No. 26

Schedule proposal and resources required for the implementation of the **Project COMET**

Expenditures, resources, financing sources			Costs (k$) Resource requirements	Proposals of the Laboratory on the distribution of finances and resources		
				2022	2023	2024
Expenditures		Computers (Simulation, data analysis)	30	10	10	10
		Laboratory electronic devices	110	30	30	50
		Materials and Equipment for: - The R&D and construction of CRV modules (scintillation strips, SiPM, fibers and other components), - The straw tubes R&D, straw tubes production and prototype creation (equipment for straw tube stand, optical sensors, pressure sensors, printing plastic for the 3D, other components). - The R&D and construction of ECAL.	190	70	70	50
Required resources	Standard hour	Resources of: - Laboratory design bureau; - JINR Experimental Workshop; - Laboratory experimental facilities division; - electron accelerator; reactor	*600 h* *900 h* *1050h*	*200 h* *300 h* *350 h*	*200 h* *300 h* *350 h*	*200 h* *300 h* *350 h*
Financing sources	Budgetary Resources	Budget expenditures including foreign-currency resources.	690	230	230	230
	External resources	- Grant of the Plenipotentiary of Georgia	30	10	10	10
		- Program of the JINR-Belarus Cooperation	15	5	5	5
		- Grant of the Plenipotentiary of Kazakhstan	15	5	5	5

PROJECT LEADERS V.V.Glagolev, Z. Tsamalaidze

Form No. 29

Estimated expenditures for the **Project COMET**

	Expenditure items	Full cost	2022	2023	2024
	Direct expenses for the Project				
1	Accelerator, reactor	*1050 h*	*350h*	*350h*	*350h*
2	Computers	-	-	-	-
3	Computer connection	-	-	-	-
4	Design bureau	*600 h*	*200 h*	*200 h*	*200 h*
5	Experimental Workshop	*900 h*	*300 h*	*300 h*	*300 h*
6	Materials (k$)	190	70	70	50
7	Equipment (k$)	140	40	40	60
8	Construction/repair of premises	-	-	-	-
9	Research operation fee (k$)	60	20	20	20
10	Travel allowance (k$)	300	100	100	100
	Total direct expenses (k$)	690	230	230	230

PROJECT LEADERS

LABORATORY DIRECTOR

LABORATORY CHIEF ENGINEER-ECONOMIST

16. APPENDIX: Additional details of the project

Based on the purpose Phase-I, the detector system is very similar to those, which will be employed in Phase-II, and acts as a prototype for the Phase-II detectors.

During Phase-I running, will be used the detector system which consists of the cylindrical detector system (CyDet), the Straw-Tracker, the electron calorimeter (ECAL), and Cosmic Ray Veto (CRV) system.

16.1 The Cylindrical Detector System (CyDet)

The CyDet is the main detector system for the $\mu-e$ conversion search in COMET Phase-I. It consists of a cylindrical drift chamber (CDC) and a cylindrical trigger hodoscope (CTH). Fig.6 shows a schematic layout of the CyDet. It is located after the Bridge Solenoid (BS) in the muon transport section, and installed inside the warm bore of a large 1T superconducting Detector Solenoid (DS) and around the stopping target.

This detector has been adopted for Phase-I as there is no downstream curved solenoid electron transport and so most beam particles that do not stop in the muon-stopping target will go downstream and escape from the detector region without leaving any hits in the detector system.

A key feature of COMET is to use a pulsed beam that allows for the elimination of prompt beam backgrounds by looking only at tracks that arrive several hundred nanoseconds after the prompt beam flash. Therefore, any momentum-tracking devices must be able to withstand the large flux of charged particles during the burst of “beam flash" particles.

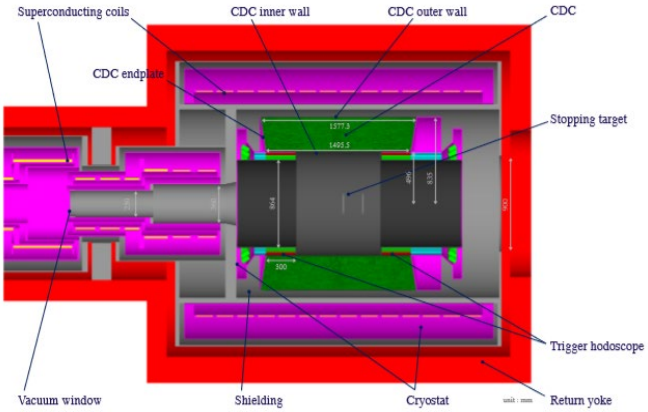

Fig.6 Schematic layout of the CyDet detector.

The radii of the inner and the outer walls are chosen to avoid DIO electrons with momentum less than 60 MeV/*c* from hitting the CDC and to fully cover the tracks of 105 MeV/*c* signal electrons. The walls are made from carbon fiber reinforced plastic (CFRP); the inner wall is 0.5 mm thick and the outer wall 5 mm. The inner and outer walls have thin aluminum foils glued inside them to eliminate charge-up on the CFRP. The endplates are conical and about 10 mm thick. Trigger hodoscopes are placed at both the upstream and downstream ends of the CDC.

The detector is designed to avoid high hit rates due to beam particles, DIO electrons, and low-energy protons emitted after the nuclear capture of muons. Among the small fraction of particles, which eventually enter the CDC and leave hits, DIO electrons and low energy protons dominate. The protons are easily identified, because the energy deposits in the CDC cells is about 100 times larger than that of similar-momentum electrons. To achieve the required sensitivity for Phase-I, the momentum resolution must be about 200 keV/*c* for 105 MeV electrons. At this energy, the

momentum resolution is dominated by multiple-scattering. Consequently, the CDC must be a low-mass detector and this dictates the construction and the choices of cell configuration, wires, and the gas mixture.

The hit rates of each CDC cell at different layers from DIO electrons from stopped muons were estimated. The rate decreases quickly at deeper CDC layers, since the DIO momentum spectrum drops as a function of an electron momentum. The time-averaged rate for the innermost sense wire is at most 4 kHz/cell, yielding an instantaneous rate of about 12.5 kHz/cell allowing for the duty factor of the J-PARC MR proton beam cycle, which is about 3. This implies a hit occupancy for one bunch cycle of 1.17 μs of about 1.5 %.

Using the results from the AlCap experiment at PSI the time-averaged hit rate on a single cell from proton emission from muon capture is estimated to be 1.4 kHz.

Other sources of hits following nuclear muon capture, such as bremsstrahlung photons, muonic X-rays, neutrons from nuclear muon capture, γ-rays from the final state nucleus have also been considered. The CDC occupancy is caused by stopped muons, which result in a total occupancy of between 7% and 10%.

The conclusion from the prototype studies is that the He:i-C_4H_{10} (90:10) gas mixture satisfies the requirements for the momentum resolution about 200 keV/c for 105 MeV electrons, efficiency of 99% and spatial resolution about 3 mm.

16.2 Straw Tracker

Since the momentum of the electrons from $\mu^- \rightarrow e^-$ conversion is as low as 105 MeV/*c*, the intrinsic momentum resolution is dominated by multiple scattering of electrons in the tracker material. Therefore, reduction of a total mass of the tracking detector and placing it in a vacuum environment are of great importance. For these requirements, a straw-tube gas wire chamber technology has been selected for the tracker.

The overall structure of the Straw Tracker (ST) is schematically shown in Fig.7. Each of the five tracker super-layers, or “stations”, consists of four planes; two to measure the *x* coordinate and two to measure the *y* coordinate. Each pair of planes is staggered by half a straw diameter in order to resolve any left-right ambiguities. Each layer is constructed as a stand-alone unit and mounted on the detector frame, which is inserted and removed from the DS on rails and linear bearings. A spare layer will also be built. Anode wires, made of gold-coated tungsten, are extracted via a feedthrough into the gas manifold as shown in Fig.7. The anode wires are held at high voltage and the straw wall is grounded, to act as the cathode. A gas mixture of 50%-Ar and 50%-C2H6 is provided from this gas manifold to the straw tube. The straws have a diameter of 9.8 mm, range in length from 692 to 1300 mm, and are mounted on aluminum ring supports.

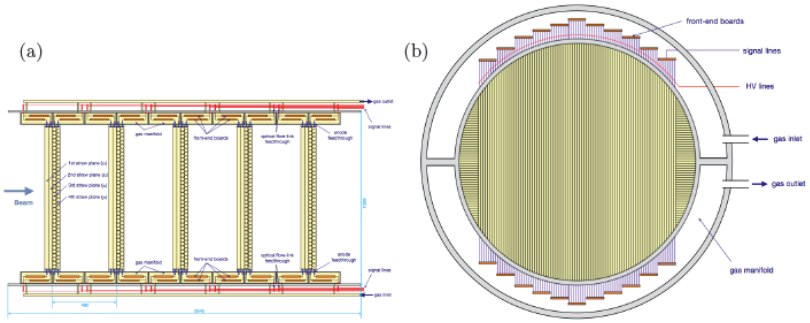

Fig.7 Schematic view of the Straw Tracker; (a) Side view (the straw dimensions is scaled by a factor of three for clarity) and (b) cross-sectional view of a plane.

A new method of straw production, which does not require multiple over-woven layers, has been developed by the JINR-COMET group using experience of the NA62 experiment at CERN [24]. In this method, a single layer is rolled and attached to itself in a straight line using ultrasonic welding. It allows the straws to be pre-tensioned at 1 kg_F, and guarantees constant tension over time. The seam width is about 500 μm, which is small enough to maintain the circular shape of the cross-section against any pressure differences. It also crucially allows the amount of material used in the tracker, which is dominated by the straw wall thickness, to be reduced. Following R&D of the JINR-COMET group, 9.8 mm-diameter straws with 20 μm thick Mylar walls and 70 nm aluminum deposition, as shown in Fig.8 were tested and found sufficiently robust.

Fig.8 Sample tubes of 20 μm-thick walls with 70 nm-thick aluminum deposition.

The straw tracker to be developed for Phase-I will make direct measurements of the particles in the muon beam line, and the rate of particle production (in particular anti-protons), as a function of beam energy and other backgrounds. It will be placed inside the vacuum vessel and the DS, which has a field strength of 0.8−1.1 T. The detector will provide a precise measurement of a particle's momentum and its identity, through *dE/dx*, *E/p* and the time of flight information in combination with the calorimeter. For Phase-I many kinds of particles will reach and enter the DS. For both phases, the volume inside the magnet will be evacuated to enable good-quality measurements of the beam particles in Phase-I and to minimize the amount of material in Phase-II. The required momentum resolution is ≤ 150 keV/c (RMS), spatial resolution is ≤ 150 μm for 100 MeV/c electron.

16.3 Electron Calorimeter (ECAL)

The electron calorimeter (ECAL) is one of the most important parts of the COMET setup, from which depends the possibility of implementing the tasks of the whole experiment. The ECAL system consists of segmented scintillating crystals. It is placed downstream of the ST to measure the energy of electrons with good resolution and hence add redundancy to the electron momentum measurement. It will also provide an additional hit position on the electron track trajectory and provide the trigger signals.

The specifications for the ECAL are determined by its requirements for Phase-II running, which are an energy resolution of better than 5% at 105 MeV and a cluster position resolution that is better than 1 cm. This is necessary to allow comparison of the position of the energy deposit to the extrapolated trajectory of a reconstructed track, and will enable the shower topology to be used also to discriminate electrons from neutrons and low-energy photons. A timing resolution better than ~ 0.5 ns is required to ensure that energy deposits in the calorimeter are in time with events reconstructed in the tracker. The crystals need to have a good light yield, high radiation

resistance, and fast response and decay times in order to reduce pileup. A schematic layout of the ECAL system is shown in Fig.9.

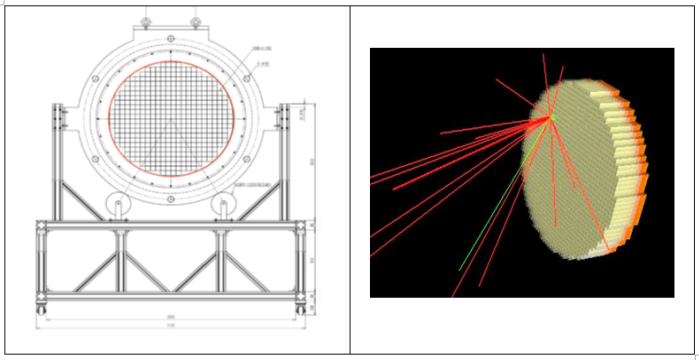

Fig.9 A schematic layout of the electron calorimeter system. The matrix structures inside the red circle represent the LYSO crystal array.

Taking into account both performance and cost, LYSO (lutetium-yttrium oxyorthosilicate, $Lu_{2(1-x)}\,Y_{2x}\,SiO_5$) has been chosen for the ECAL. High segmentation is required both to reduce pileup and provide good position information. The ECAL will consist of crystal modules which have a 2×2 cm^2 cross-section and whose length is 12 cm corresponding to 10.5 radiation length. The ECAL covers the cross-section of the 50 cm radius detector region and 1920 crystals are needed.

The photon detectors for the ECAL must be able to operate in the 1 T magnetic field, have a high quantum efficiency around the wavelength range of LYSO scintillation and excellent linearity. The Hamamatsu S8664-1010 avalanche photodiode (APD) with an active area of 10×10 mm^2 satisfies these requirements.

The basic unit of the ECAL is a 2×2 crystal matrix module with 480 modules to cover the full cross-section of the detector region. A prototype module is shown in Fig.10.

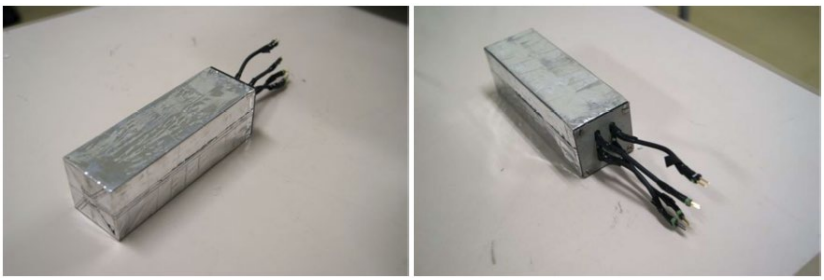

Fig.10 A prototype of the 2×2 crystal matrix module (without the preamplifier board).

A polished crystal is first wrapped by a reflector film (3M ESR) together with a silicone rubber optical interface and a PCB on which the APD (Hamamatsu S8664-55 APD) is attached. An LED with a wavelength similar to that of the LYSO scintillation photon (420 nm), is also placed on the PCB and is used to flash light for monitoring purposes. This one crystal structure is then wrapped by a layer of Teflon tape. Four wrapped crystals are then used to construct the 2×2 matrix module, which is wrapped by an Al-Mylar. The modules are further arranged to form a super-module.

16.4 Cosmic-Ray Veto (CRV)

Cosmic Ray muons (CRM) can decay in flight or interact with the materials around the area of

the muon-stopping target and produce signal-like electrons in the detector region. In order to have control over this background, a Cosmic Ray Veto (CRV) system is required for COMET. The CRV has to identify cosmic ray muons with an average inefficiency that is lower than 10^{-4}.

For COMET Phase-I, two types of cosmic-ray shielding will be used: passive and active. The passive shielding consists of concrete, polyethylene, and lead, as well as the iron yoke of the DS. The flux of low-angle cosmic particles is also attenuated by the surrounding sand as the detector is located underground.

The active shielding is provided by a CRM detection system covering the CyDet area. Detailed studies of CR-induced backgrounds indicate that the BS area must also be covered by a CRV, because interactions of CRM in the BS could produce electrons that scatter off the BS and enter the CDC, hit the CTH and mimic signal events. A suppression factor of 10^4 is needed for this CRM background and it is obtained by using - in the offline analysis - the signature left in the CRV by the CRM. The active veto system covering the CyDet is made of scintillator-based detectors, whereas Glass Resistive Plate Chambers (GRPC) are envisaged in the BS area.

The CyDet CRV has four layers of active material. Its basic element is a strip made of a polystyrene-based organic scintillator. This detector is named the Scintillator-based Cosmic Ray Veto (SCRV).

The principle for particle detection and the general design of a single SCRV channel are shown in Fig.11. The single scintillator strip has a cross-sectional area of 0.7×4 cm^2 and a length up to 360 cm. It is made of polystyrene (Styron 143E) acting as ionization and photon carrier medium with 2% scintillating fluors (p-terphenyl) and 0.05% POPOP.

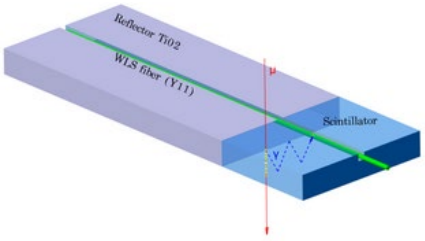

Fig.11 The design for a single channel and the principles of particle detection.

SCRV strips are read out by wavelength-shifting (WLS) fibers, which transport light to the photodetectors. The use of WLS fibers is necessary in order to compensate for the short attenuation length of the scintillators and to optically connect the scintillators to the photodetectors. The WLS fiber is placed along the strip length in a surface groove of a rectangular shape. Several different groove dimensions have been studied and the optimal one was determined to be 1.5×3.5 mm^2. A good optical coupling between the scintillator strip and the WLS fiber is ensured by the use of a highly transparent optical glue, BC600 (Bicron optical cement).

The WLS fibers are read out by Silicon Photomultiplier (SiPM) detectors at both ends. The double-ended readout design allows one to determine the muon impact point along the strip with an accuracy of a few cm, by measuring the time difference between the SiPM signals, or by measuring the difference of light yield of both ends. Consequently, the required spatial accuracy of a few cm is achieved without introducing longitudinal segmentation. As CDC will be able to provide much better tracking of cosmic muons, this spatial resolution of CRV is enough.

The region around the BS that requires active shielding has a surface of 3×1900×600 mm^2. Simulations indicate that this area suffers from a larger neutron contamination compared with that

affecting the CyDet CRV.

GRPCs are a natural candidate for operating in such high neutron flux areas; they can be built to the required size and provide an uniform tracker, without dead areas between adjacent active volumes. These are thin detectors of less than 3.6 mm, with nanosecond time resolution, operated at average efficiencies of 95% and with an intrinsic position resolution of a few mm. The design of GRPC was envisaged for COMET Phase-I. The BS CRV is based on three trackers to be deployed on the top and the sides of the BS respectively. Each tracker is made of six GRPC modules.

16.5 Trigger Systems

Phase-I will have two distinct running modes. One with the StrECAL as main detector to measure backgrounds and characterize the beam and the other with the CyDet as main detector to search for $\mu^- N \rightarrow e^- N$. There will be distinct but similar DAQ and trigger systems for the two modes. Detectors such as a beam monitor and an X-ray monitor (to determine the muon beam profile and number of muons captured in the target, respectively) will be employed for both modes. Similarly, the CRV will provide a veto whilst running with beam (which can be applied offline), but can also provide a calibration trigger.

16.5.1 The CyDet Trigger

The main trigger when operating in CyDet mode is provided by requiring 4-fold coincidence on neighboring counters from the CTH detector. This is supplemented by using the track patterns from the CDC hits as these are quite different for high-momentum electrons (signal or DIO) than the low-momentum particle noise hits. For the CyDet component, a simple combination of hit pattern and energy deposition can yield a sufficiently fast trigger with high efficiency and background rejection power, resulting in an overall trigger rate of a few kHz**.**

16.5.2 StrECAL Trigger

In the StrECAL mode the trigger is provided by the ECAL. The energy deposition from a single track can be divided among several crystals and so a summation is necessary to reconstruct the full energy. The summed energy over crystals, which form a 4×4 square can effectively include almost all the energy deposited by electrons with energies of about 100 MeV. The basic trigger unit (cell) will therefore be a group of 2×2 crystals (one ECAL crystal module), and the total energy determined by using the sum of an array of 2×2 trigger cells referred to as a trigger group. The energy resolution of the ECAL pre-trigger system is measured 4.5 MeV for 105 MeV electrons, which is sufficient for trigger performance. The effectiveness from simulation with at least a 10^6 DIO rejection for around a 90 % conversion electron detection efficiency.

A StrECAL cosmic trigger is also required for tests and calibrations when not running with beam. It will be based on the cosmic veto system with simple coincidences of hits in different layers of bars close to each.

16.5.3 Trigger Rate

For the CyDet trigger the deadtime is less than 1 μs and hence the actual maximum trigger rate in CyDet mode is 440 kHz, whereas for the StrECAL trigger the deadtime is 36.7 μs that leading to a maximum trigger rate of 26 kHz. However, the effective trigger rate is dictated by the DAQ system, which is not greater than 20 kHz.

16.6 COMET Phase - α

16.6.1 Introduction and Purpose

The COMET collaboration intends to carry out a low beam intensity run (Phase-*α*) in 2022. The proton beam power in COMET Phase-*α* is assumed to be 260 W with a beam spill cycle of 9.2 seconds and beam time structure of 1.17–1.75 *μ*sec bunch-to-bunch time widths. The acceleration scheme and proton beam characteristics such as the bunch length and beam extinction factors are identical to those of COMET Phase-I. The number of bunches is 7.6×10^5/sec. Each bunch contains 4.9×10^6 protons, resulting in 1.9×10^{12} protons/spill.

The purpose of this run is to understand the proton beam transported to the COMET experimental area and *π*/*μ* production yield in the backward direction at 8 GeV before the Pion Capture Solenoid (PCS) is installed in the COMET primary beam line area. This enables us to measure the proton beam characteristics and *π*/*μ* production with less ambiguity albeit with a significantly lower secondary beam yield. A thin (1 mm thick) graphite plate is used as a pion production target surrounded by radiation shielding. A beam diagnostic detector will be located around the target area. The beam extinction measurement in the COMET experimental area, which the primary proton beam reaches via a transport line from the J-PARC Main Ring (MR), will also be conducted using semi-conductor detectors being developed in the collaboration. Some of the secondary particles produced at the graphite target in the backward direction will enter the Transport Solenoid (TS) and are transported to the detector region of the COMET experimental area. Secondary-beam measuring detectors will be set in the COMET experimental area and measure the beam phase space with possible particle-identification (PID).

16.6.2 Setup for Yield Estimation

The particle yield estimation has been performed by simulation using Geant4, and a fully detailed geometry a realistic magnetic field has been produced. Fig.12 shows the simplified geometry.

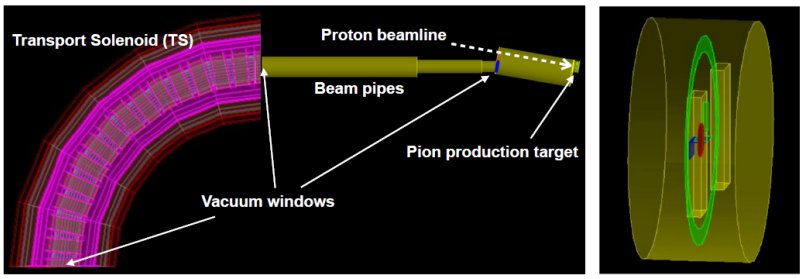

(a) Entire geometry (b) Around the target

Fig.12 The simplified simulation geometry. (a) It consists of only the components associated with the secondary beam from the pion production target. There are three titanium vacuum windows, each with a thickness of 500 *μ*m. (b) The volume in red is the 1 mm-thick graphite target, and the surrounding components form its support structure.

Most of it adheres to the most current design, while the bridge section between the beam pipe and the TS is in a simplified form. At the position of the rightmost pipe, a graphite target disk is fixed in a support structure. For the magnetic field, only the field in the TS region was implemented, having been imported from the Phase-I field map. This also contains the dipole correction field map, which has been optimized for Phase-I.

In simulation study with this setup, a geometry was created with all components incorporated

according to their current designs. The magnetic field was also calculated specifically for the Phase-α setup. Fig.13 shows the geometry up to the TS, and the magnitude of the magnetic field. Radiation-blocker materials are also positioned around the upstream beam pipes.

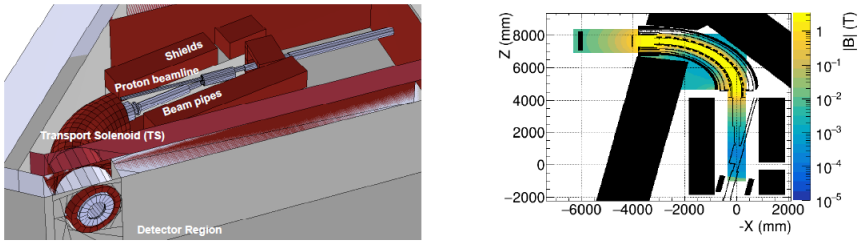

(a) Entire geometry (b) Field map

Fig.13 (a) The geometry of Phase-α. (b) The magnetic field map specifically for Phase-α.

We ran 10^{11} proton-on-target (POT) events with the simplified setup and estimated the yields for different types of secondary particles. Table 1 lists the numbers of $e^{\pm}$, $\mu^{\pm}$, $\pi^{\pm}$, and p that reach the TS entrance and exit. As a comparison, the numbers are roughly 10^5-10^6 times smaller than those for Phase-I, owing to the thin pion production target and the missing PCS. There are no large differences between particles and antiparticles for each type. This is because the particles that can enter the TS do not have a high transverse momentum, which is necessary for electric charge separation in the curved solenoid. Fig.14 shows the momentum distributions at the exit. In particular, that of μ^- contains our range of interest from 40 to 60 MeV/c, which is required for the muons to stop in the aluminum target disks.

Table 1: Yields per POT of the secondary particles, which reach the entrance and exit of the transport solenoid (TS).

Particle	TS entrance	TS exit
e^-	8.3×10^{-8}	4.6×10^{-8}
e^+	3.2×10^{-8}	3.3×10^{-8}
μ^-	2.0×10^{-8}	6.9×10^{-9}
μ^+	2.8×10^{-8}	1.1×10^{-8}
π^-	5.2×10^{-8}	1.7×10^{-9}
π^+	7.3×10^{-8}	2.8×10^{-9}
p	1.6×10^{-7}	4.0×10^{-10}

Although the simulation statistics obtained for the full setup are still low at present, at less than 10^9 POT events, the results are consistent with those made with the simplified setup, within statistical uncertainties. More simulation data are being produced for more detailed evaluations.

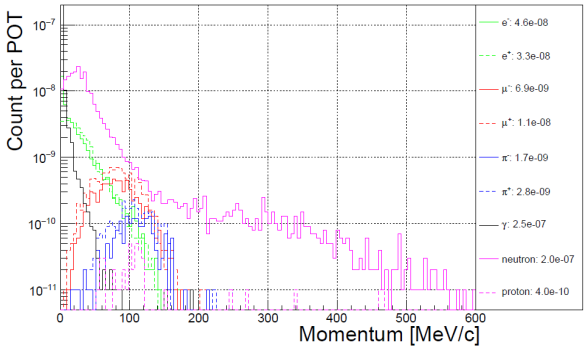

Fig.14 Momentum distributions of several secondary particle types at the transport solenoid exit. The particle type for each line is shown together with the yield per POT.

16.6.3 Measurements method and setup for PID performance

The PID performance at Phase-*α* between e^-, μ^-, and π^- has been studied by implementing realizable detectors in the simulation. They are, as shown in Fig.15, a plastic scintillator hodoscope, measures d*E*/d*x* and ECAL, measures energy deposits. Also the time-of-flight (TOF) is also determined using both detectors. Together, they are used to measure the kinematic distributions of the incoming particles, such as timing and energy, but those variables are also made use of for PID.

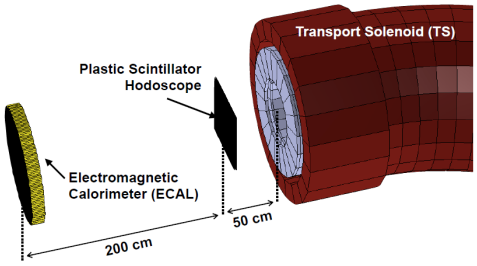

Fig.15 Setup of the detectors, which lie beyond TS.

For this study, detector hits were sampled over 8×10^8 POT events. However, the Phase-I geometry was used for the simulation, except for the detectors because the Phase-*α* beam pipes around the pion production target had not been implemented in the simulation at the time. Although the momentum distribution of the beam particles does differ from Phase-*α* because of this, the momentum range of interest is covered, and the results are adequate for the purposes of this study. Note that detector resolutions are not taken into account, nor hit-rates and the effects of pile-up.

In the analysis, to identify the particle types the following three variables are used:

- d*E*/d*x* - the energy deposit in the hodoscope,
- Prompt energy - the total energy deposit within 10 nsec of the particle hit time in the ECAL,
- Time-of-flight (TOF) - the hit time difference between the hodoscope and the ECAL.

Figure 16 shows the resulting PID efficiency for each particle type as a function of momentum. The efficiency is defined as N_{ID}/N_{hit}, where N_{hit} is the number of particles within a specific momentum range that hit both detectors without decaying between them, and N_{ID} is the number amongst those that are correctly identified. Evaluated PID efficiency curves for e^-, μ^-, and π^-:

- e^-: Good ~ 100%,
- μ^-: Good > 90% but drops at high momentum,
- π^-: Still low over the range.

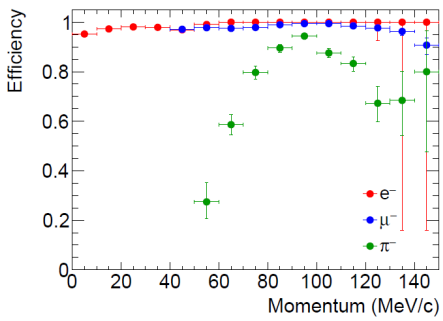

Fig.16 PID efficiency for each of e^-, μ^-, and π^- as a function of momentum.

16.7 Simulation and Data Analysis

Development of the straw tracker and calorimeter systems required a lot of simulation work. The corresponding results are presented in the Technical Design Report for Phase-I of COMET [1]. In particular, the values of efficiency and space resolution in different conditions: for the tubes of different diameters, wall thicknesses and gaps between the tubes, for the straw tracker have been established. Similarly, the calorimeter simulation has been done for two types of crystals, GSO and LYSO using the real optical parameters. Among others, simulation of light outputs and light collection with different reflecting materials also has been performed. Simulated energy resolution was found to be better for the LYSO type what has been confirmed later experimentally.

A dedicated simulation has been done with the aim to optimize the operation of the J-PARC Main Ring in order to achieve very low extinction factor, below 10^{-9}, what is the must for COMET.

A very essential task is working in the COMET software - ICEDUST, in particular, to simulate the response of the straw tracker.

Also work on simulation was done in Garfield++. Some of the purposes are to obtain drift lines in a 3-dimensional view and make changes in the algorithm for construction of isochronous drift lines in Garfield ++ taking into account the design features of the COMET experiment.

The Geant4 simulation of the optimal structure of the segmented calorimeter for the COMET experiment was made. The simulation of the electromagnetic calorimeter was included in the framework ICEDUST, which is adopted framework for any COMET software activity.

The data from the calorimeter prototype beam test has been analyzed independently in Japan, based on the similar analysis. Both analyses have led to the conclusion about a better performance of the LYSO crystals.

Since the optical model of LYSO crystal is not implemented in the GEANT4, an optical model of LYSO crystal was developed. To obtain the optical model of the crystal, the SLitrani package and measurements of the main optical parameters of the crystal performed on the setup were used. To verify the G4 optical model, G4 simulation of LYSO crystal was performed.

The simulation of the optimal structure of the ECAL calorimeter was performed based on the Geant4 package by using the optical model of LYSO crystal. The simulations were made taking into account the real conditions of the COMET experiment: 1) the calorimeter was located in 1 T uniform magnetic field; 2) electron beam energy spread was 105 ± 0.5 MeV, and beam spot was 1 cm^2 ± 1 cm; 3) the crystals were wrapped with two layers of Teflon (thickness 60 μm). These simulation conditions are similar to the conditions under which the Beam Test in Tohoku (except the magnetic field) of calorimeter prototype for LYSO and GSO crystals was performed. Thus, the obtained Geant4 optical model can be used to simulate the calorimeter and for data handling of the COMET experiment [25].

In the future, we are planning to enlarge our scope of works on simulation and analysis in order to be ready for physics analysis of the COMET data from J-PARC.